Materials Letters 214 (2018) 272–275

Contents lists available at ScienceDirect

Materials Letters

journal homepage: www.elsevier.com/locate/mlblue

Sol-gel-controlled synthesis of hollow TiO_2 spheres and their photocatalytic activities and lithium storage properties

Yan Bao [a,b,*], Qiao Ling Kang [a,c], Chao Liu [d], Jian Zhong Ma [a,b,*]

[a] College of Bioresources Chemical and Materials Engineering, Shaanxi University of Science and Technology, Xi'an 710021, China
[b] Shaanxi Research Institute of Agricultural Products Processing Technology, Xi'an 710021, China
[c] National Demonstration Center for Experimental Light Chemistry Engineering Education, Shaanxi University of Science & Technology, Xi'an 710021, China
[d] Shaanxi Collaborative Innovation Center of Industrial Auxiliary Chemistry and Technology, Xi'an 710021, China

ARTICLE INFO

Article history:
Received 2 November 2017
Received in revised form 8 December 2017
Accepted 9 December 2017
Available online 11 December 2017

Keywords:
TiO_2 hollow spheres
Sol-gel synthesis
Photocatalytic activities
Lithium-ion battery

ABSTRACT

A novel ammonia and triethanolamine assisted sol-gel synthesis method was developed to fabricate TiO_2 hollow spheres (THS). The hollow structure of TiO_2 could be easily controlled by adjusting the amount of ammonia and triethanolamine. Photocatalytic activities of the THS were evaluated by the photodegradation of Rhodamine B (RhB). The results show that the anatase/rutile mixed-phase THS obtained from 850 °C thermal treatment exhibits higher photocatalytic activity than Degussa P25 (commercial TiO_2 photocatalyst). In addition, electrochemical measurements demonstrate that the mixed-phase THS have potential applications in lithium-ion battery.

1. Introduction

TiO_2 has been widely investigated for the past decade due to its wide potential applications in catalysis, dye-sensitized solar cells, sensors and electrode materials for lithium batteries [1]. THS have attracted considerable interest owing to their high surface area and unique hollow structure [2,3], which can be easily obtained after removing the template core. In addition, there are two main approaches to prepare the shells: layer-by-layer self-assembly [4] and sol-gel nanocoating [5]. The sol-gel nanocoating is widely used due to its simplicity and high efficiency. However, it is well-known that the hydrolysis and condensation of titania precursors are too fast to control in sol-gel nanocoating. So inhibitor agents used to slow down the rate of hydrolysis and condensation of titania precursors are needed. Inorganic acids (e.g., nitride acid [6]) and organic complexing agents (e.g., acetyl acetone [7]) are often considered as inhibitors. But the use of a single agent only offers limited control over the sol-gel process of titania precursors in various conditions.

Here, ammonia and triethanolamine were first employed to control the sol-gel process. The active hydroxyl of triethanolamine could induce the transesterification of tetrabutyl titanate to form triethanolamine modified tetrabutyl titanate, which restrained the hydrolysis and condensation of titania precursors [8]. Then the modified tetrabutyl titanate could be dissociated by the more active ammonia, and the ammonia-catalyzed sol-gel process could take place to generate titania sols. Based on the above reasons, the THS were successfully prepared thanks to the use of ammonia and triethanolamine (Supplementary Fig. S1). The THS show a higher photocatalytic activity than P25 provided by Degussa company, and exhibit a potential application in lithium energy storage.

2. Experimental section

2.1. Synthesis of TiO_2 hollow spheres

13.33 g of polystyrene (PS) latex and ammonia were added to 100 mL of ethanol under stirring, then 4 mL of ethanol solution containing a certain ratio of tetrabutyl titanate (TBT) and triethanolamine was added dropwise into the suspension. The resulting reaction was conducted at 80 °C for 6 h. TiO_2 samples with different surface crystalline phases were prepared by calcining in air at 500 °C (anatase phase), 850 °C (anatase/rutile mixed-phase) and 1000 °C (rutile phase), respectively. The morphology and structure could be controlled by adjusting the amount of ammonia and triethanolamine (Supplementary Table S1).

* Corresponding authors at: College of Bioresources Chemical and Materials Engineering, Shaanxi University of Science and Technology, Xi'an 710021, China.
E-mail address: baoyan@sust.edu.cn (Y. Bao).

https://doi.org/10.1016/j.matlet.2017.12.038
0167-577X/

2.2. Material characterization

The morphology and microstructure of the samples were observed using a Field Emission Scanning Electron Microscope (SEM, S4800, Japan) and Transmission Electron Microscope (TEM, Hitachi, H-7650, Japan). X-ray diffraction (XRD) patterns were collected on a D/Max 2200PC diffractometer with a CuKα radiation (λ = 0.15418 nm). UV spectra were recorded on a Cary 5000 spectrometer at room temperature.

3. Results and discussion

The morphology and structure of THS were characterized by SEM and TEM (Fig. 1a–c). The titania shell is homogenous and complete, which is composed of primary nanoparticles to make its surface rough and porous. It can be seen that THS have a remarkable cavity from the TEM image. The size distribution of the hollow spheres shows that they have a uniform diameter of about 300 nm (Supplementary Fig. S2). The BET specific surface area of THS is 58.3 $m^2 g^{-1}$. The larger specific surface area originates from the small size, ultrafine nanocrystals, and hollow porous structure of the THS. In addition, the average pore size of THS is approximately 13.3 nm (Supplementary Fig. S3).

Fig. 1d shows the XRD patterns of TiO_2 and P25 samples. The crystalline phase of THS has been modified by the calcination temperature. The crystalline phase of the TiO_2 sample calcined at 500 °C is pure anatase, which has an interplanar spacing of 0.352 nm (Fig. 1e). Upon increasing the temperature to 850 °C, the anatase TiO_2 transformed gradually into the rutile phase, with the shell forming an anatase-rutile junction (Fig. 1e). In brief, the mixed-phase THS will be a highly desirable structure for high-performance photocatalysts [9]. When the temperature is increased to 1000 °C, the surface region is completely transformed from the anatase to the rutile phase, which is also indicated by an interplanar spacing of 0.324 nm corresponding to the (1 1 0) planes of rutile TiO_2 (Fig. 1e). The P25 catalyst is presented as a reference to confirm the phase constituents of the mixed-phase TiO_2. Moreover, the ratio of rutile phase in the as-prepared mixed-phase TiO_2 hollow structure is larger than that in the P25. The specific surface area and pore volume decrease with the crystalline phase of TiO_2 transformed from anatase to rutile, which is proved by nitrogen desorption/adsorption isotherms (Supplementary Fig. S3 and Table S2). This can be explained by the increase of the shell impactness of THS along with the increase of the calcination temperature. In addition, we also proved that the morphology and structure of the THS can be controlled by adjusting the amount of ammonia and triethanolamine (Supplementary Figs. S4 and S5).

The photocatalytic activity was evaluated by monitoring the degradation of RhB under UV irradiation versus time (Fig. 2a and b). In the blank experiment (without catalyst), only 9% RhB is decomposed after UV irradiation for 120 min, but the degradation rates are notably enhanced in the presence of photocatalysts after a similar irradiation time. The relative photocatalytic activities of the catalysts are in the following order: mixed-phase THS > anatase THS > P25 > rutile THS. In particular, the RhB molecules can be completely decomposed in the presence of the mixed-phase THS after only 90 min of irradiation with UV light. This is attributed to the fact that the electron-hole pair diffusion from anatase to rutile is vital to decrease the combination

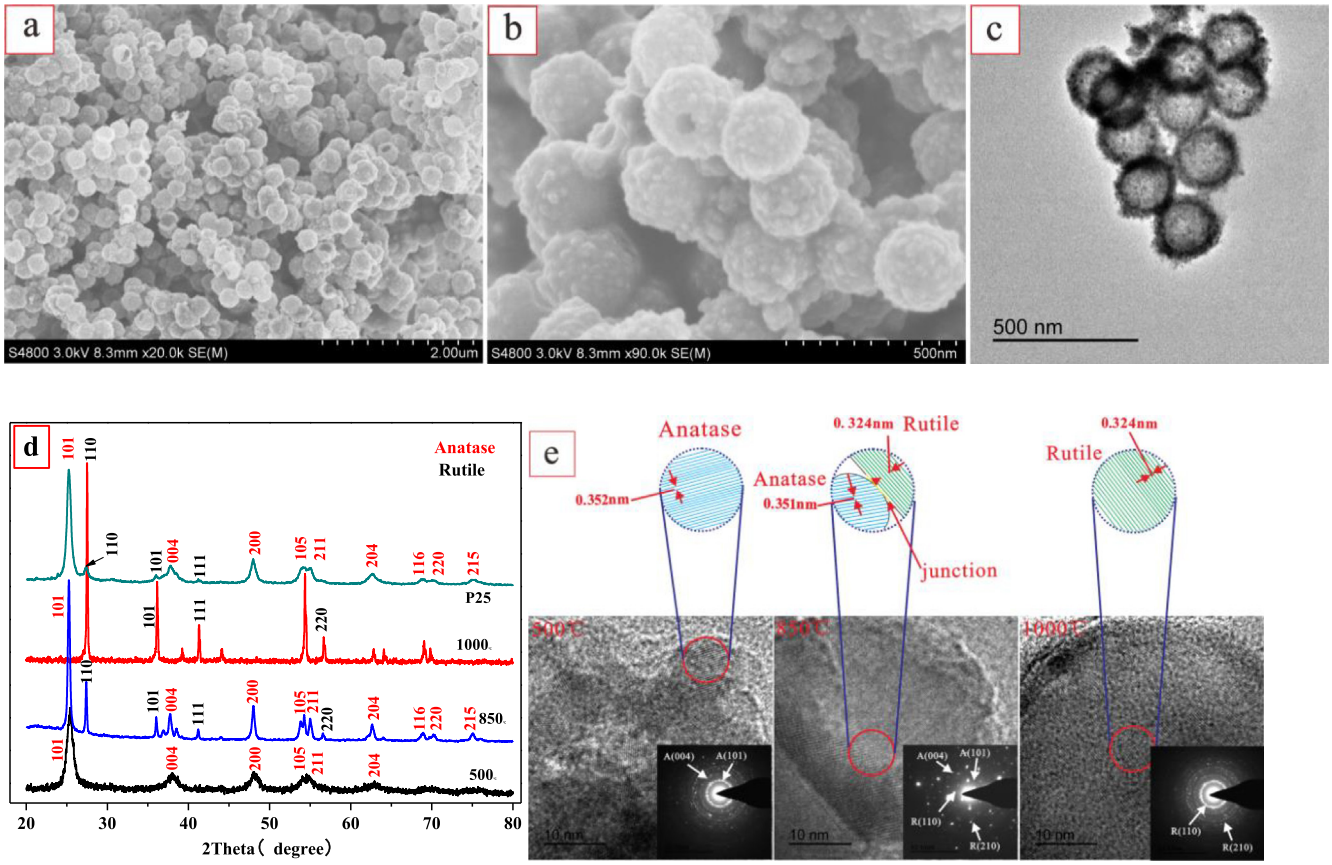

Fig. 1. SEM images of samples with the amount of triethanolamine and ammonia (a and b) 2 mmol and 272 mmol, the corresponding TEM image (c), XRD pattern of samples (d) and HRTEM images of samples (e).